

# Microstructural characterization of silica aerogels using scanning electron microscopy

G. M. PAJONK, A. VENKATESWARA RAO\*, N. N. PARVATHY and E. ELALOUI  
*Laboratoire d'Application de la Chimie à l'Environnement (LACE) CNRS, Université Claude Bernard, Lyon I, 43 boulevard du 11 Novembre 1918, 69 622 Villeurbanne Cedex, France*

In this paper the experimental results of microstructural characterization of silica aerogels using scanning electron microscopy (SEM) are reported. In order to understand the reasons for shrinkage, opacity and cracking of the aerogels, detailed SEM observations have been made on the aerogels prepared using various molar ratios of precursors, catalysts and solvents; gel ageing periods and supercritical drying conditions. It has been observed that strong acidic catalysed gels resulted in smaller pore and particle sizes, and hence more transparent but readily cracked aerogels; whereas weak-basic catalysed gels gave larger pore and particle sizes, and hence slightly less transparent and monolithic aerogels. Microstructures of very low density ( $0.05 \text{ gm cm}^{-3}$ ) gels indicate that the gels form a highly crosslinked polymer network and, then, the spherical particles form on the network at higher aerogel densities. Gel ageing resulted in neck growth between  $\text{SiO}_2$  particles. Precise control of pore and particle sizes using sol–gel parameters have been found to be necessary in order to obtain highly transparent and monolithic silica aerogels. In addition, autoclave heating and solvent evacuation rates of around  $25^\circ\text{C h}^{-1}$  and  $4 \text{ cm}^3 \text{ min}^{-1}$ , respectively, resulted in the best quality silica aerogels in terms of monolithicity and transparency.

## 1. Introduction

Since the early 1970s there has been great interest in silica aerogels because they are extremely porous and transparent materials (in the visible range) consisting of  $> 95\%$  air and  $< 5\%$  silicon dioxide. Due to their high porosity (up to  $99.8\%$ ) [1] and very large inner surface area ( $1600 \text{ m}^2 \text{ gm}^{-1}$ ) [2], they are used as catalyst supports [3–6], membranes, fillers and reinforcement agents [7], filters for purification of polluted air and water [8, 9] gellifying agents [4], containers for micrometeorite particles in space [10] and liquid rocket propellents [4]. They are being tested, in place of chlorofluorocarbon (CFC) blown polyurethane foam, for superthermal insulation in solar ponds and cookers, double glazing [11], refrigerators and thermos flasks [12]. Owing to their very low refractive indices [1.01 to 1.1], they are extensively used as Cerenkov radiation detectors in nuclear reactors and high energy physics [13–15]. Since the velocity of sound in silica aerogel is around  $100 \text{ ms}^{-1}$ , they are used as acoustic impedance devices [16]. However, one of the most important and recent applications of silica aerogels is the use of these materials as inertial confinement fusion (ICF) targets in thermonuclear fusion reactions [17–19]. Recently, silica aerogels have been used as highly efficient radioluminescent light and power sources in place of fragile vacuum systems [20].

Silica aerogels were first produced by Kistler [21] by mixing sodium metasilicate of 1.15 specific gravity and 99.9999% hydrochloric acid followed by water rinsing, alcohol substitution and supercritical drying. However, Kistler's method is very tedious and takes several weeks, and therefore Nicolaon and Teichner [22] developed a versatile process using alkoxide precursors to prepare silica aerogels within a few hours. Since then, silica aerogels have been studied for various scientific and industrial applications [23].

Recently, detailed studies have been reported on the preparation and characterization of silica aerogels [24–26]. However, it has been observed that even though supercritical drying eliminates the capillary forces that cause fracture of the aerogels, the aerogels still shrink and crack frequently in the autoclave. This is due to the fact that there are several interdependent sol–gel and supercritical drying parameters involved during the preparation of silica aerogels. Generally, cracks in the aerogels start from microcracks in the alcogels. According to the pioneering work of Scherer [27] on crack propagation in silica aerogels, the cracking depends on the permeability and solvent flow properties, which in turn depend mainly on pore and particle sizes and shapes and their distributions. Therefore, in order to understand the reasons for shrinkage, cracking and opacity of the aerogels, one has to take up systematic

\* Permanent address: Air Glass Laboratory, Department of Physics, Shivaji University, Kolhapur-416004 India.

microstructural investigations of silica aerogels using scanning electron microscopy (SEM). Although microstructural studies of aerogels using SEM have been reported briefly in [28–32], there are no reports on the influence of sol–gel and drying parameters on SEM microstructures. Hence, the present paper reports the results on the SEM studies of the aerogels prepared under various sol–gel and drying conditions.

## 2. Experimental procedure

Silica alcogels (the dispersed phase is an  $\text{SiO}_2$  skeleton and the dispersing medium is alcohol) were produced by hydrolysis and polycondensation of solvent [methanol (MeOH) or ethanol (EtOH)] diluted tetraalkoxysilane [tetramethoxysilane (TMOS) or tetraethoxysilane (TEOS)] in the presence of a basic ( $\text{NH}_4\text{OH}$ ) or acidic (HCl) catalyst. The chemicals used in the present work were of 'Pursis' grade from Fluka Co. (Switzerland). Triple distilled water was used for making catalysts of different concentrations and for hydrolysis reactions. The pH values of the sols were varied from one to ten by varying the concentrations of the catalysts. The silanes were diluted with their respective parent alcohols in order to avoid transesterification [25]. All the solutions (silane, solvent, water and catalyst) were mixed in a 250 ml pyrex beaker and the resulting sols were immediately transferred to pyrex test tubes of 18 mm outer diameter and 180 mm height, and closed air tight. After gelation, the resulting alcogels were covered with their respective solvents in order to prevent shrinkage and cracking of the alcogels. The gelation took place at a constant temperature of  $25^\circ\text{C}$ , unless otherwise specified. All the alcogels were supercritically dried in an autoclave as per the procedures described in [24, 25].

In order to obtain the best quality aerogels in terms of transparency, homogeneity and monolithicity, five sets of experiments were performed in which the sol–gel parameters: molar ratios of precursors (TMOS and TEOS), catalysts, solvents, alcogel ageing periods and supercritical drying conditions, were varied. With a view to understanding the reasons for shrinkage, opacity and cracking of the aerogels, microstructural observations were made of the aerogel samples by SEM with a Cambridge 250 MK3 scanning electron microscope. Aerogel samples were carefully cut into  $3 \times 3 \times 2 \text{ mm}^3$  at atmospheric pressure in a dustproof clean chamber. Then the samples were coated with gold containing 20% palladium, at a pressure of 1.333 Pa, in order to avoid electric charge during the SEM observations. Other coating procedures (Pt–C coating and osmium-impregnation followed by Pt coating) have been used also and the SEM microstructures are very similar to those of Au–Pd coating. It has been found that the reproducibility of the results mainly depends on obtaining the reproducible aerogel samples under various sol–gel and supercritical drying conditions. The authors have observed that the reproducibility of the aerogels is greater than 90%. In the present work, four different samples, prepared under each identical condition, have been examined and the results have been found to be very similar.

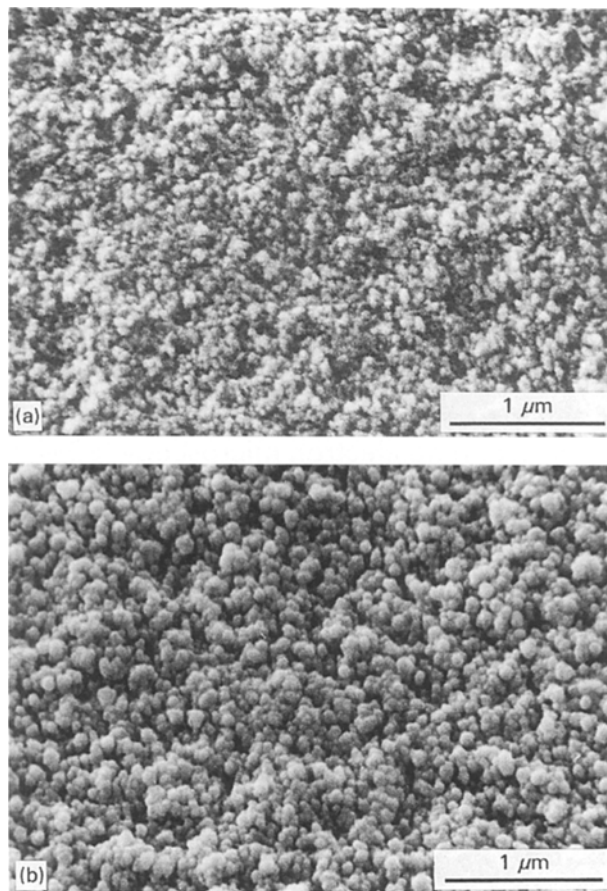


Figure 1 SEM photographs of silica aerogels prepared using (a) acidic (HCl) and (b) basic ( $\text{NH}_4\text{OH}$ ) catalysed alcogels.

## 3. Results and discussion

In order to know the effect of acidic and basic catalysts on the microstructures of silica aerogels, alcogels were prepared by keeping the molar ratio of TMOS:MeOH: $\text{H}_2\text{O}$  constant at 1:8:4, respectively, with a catalyst concentration of 0.2 N (1.4%). Sols containing acidic catalysts resulted in transparent, but cracked, aerogels. On the other hand, monolithic and transparent aerogels were obtained using basic catalysts. Fig. 1a and b shows SEM microstructures of silica aerogels using acidic (HCl,  $\text{pH} = 2$ ) and basic ( $\text{NH}_4\text{OH}$ ,  $\text{pH} = 6.5$ ) catalysts, respectively. Here, it is interesting to note that the pH values for both the acidic and basic sols are on the acidic side only. This is due to the fact that the pH values of TMOS and MeOH are on the acidic side ( $\text{pH} \approx 4$ ) and hence the pH of even 0.2 N (1.4%)  $\text{NH}_4\text{OH}$  incorporated sol has a value of 6.5. It is clear from Fig. 1a that the acid catalysed gel has smaller particles of non-uniform shape and polydispersed pores. It is known that HCl accelerates hydrolysis and retards condensation [33], leading to shrinkage and hence high bulk density with fine particles and polydispersed pores [34, 35]. On the other hand, an  $\text{NH}_4\text{OH}$  catalyst gives almost monodispersed well defined spherical particles and clusters of particles with large size pores. It is known that  $\text{NH}_4\text{OH}$  limits hydrolysis, accelerates condensation [33], and produces low bulk density with large pores and particles [34]. SEM observations (Fig. 1b) indicate that, under the present operating conditions,

SiO<sub>2</sub> skeletons seem to be formed from particulate clusters as reported in [36]. These results can also be explained by considering syneresis strain and permeability of gels.

Scherer [27] observed that the syneresis strain, ( $\epsilon_s$ ) decreases and permeability,  $D$ , increases, i.e. stress decreases, as the gel pH increases from acidic to basic. From the authors' experimental results, the limit to basic pH was put at around eight; at pH > 8 the gels cracked. In addition, the  $D$  values depend on the pore size,  $r$ , according to the Carman–Kozeny equation [37]

$$D = (1 - \rho) r_h / f_s f_T$$

where  $\rho$  is the relative density of the drained bulk network, i.e. aerogel bulk density;  $r_h$  is the hydraulic radius (defined as  $r_h = V_p / S_p$ , where  $V_p$  and  $S_p$  are the volume and surface area of the pores, respectively);  $f_s$  and  $f_T$  are factors inserted for the non-circular cross-section and non-linear path of the pores in a real material. The Carman–Kozeny equation was developed for granular materials, but it describes flow through networks and fractals also [38]. Scherer and Swaitek [39] concluded that the permeability of silica aerogel is strongly dependent on the microstructure, with the coarser base catalysed gel having a permeability ten times greater than the acid catalysed gel. This clearly indicates that cracking of the aerogels strongly depends on the shape and size of the pores of the gel.

It has been found that at constant molar ratios of MeOH:TMOS (A) and H<sub>2</sub>O:TMOS (B) of eight and four, respectively, with an alcogel ageing period of eight days, the transparency of the aerogels increases with an increase of NH<sub>4</sub>OH:TMOS molar ratio,  $C$ ; but at the same time the cracking of the aerogels also increases. It is clearly seen from the SEM observations shown in Fig. 2a and b that the higher ( $> 5 \times 10^{-2}$ )  $C$  values result in smaller pore and particle sizes; whereas lower ( $< 6 \times 10^{-3}$ )  $C$  values give larger pore and particle sizes. These observations can be explained by the fact that at higher  $C$  values the aerogels form smaller sized nanoparticles, leading to greater transparency and more cracks. Also, it has been found that at higher  $C$  values, the condensation rates are much greater, which leads to faster gelation and hence larger nucleation rates resulting in smaller particles. Prassas *et al.* [40] have also obtained cracked aerogels at higher catalyst (NH<sub>4</sub>OH) concentrations. These authors have attributed cracks to the fast condensation of the sol. Pekala [41] has observed greater shrinkage at higher catalyst concentrations in the case of organic aerogels, and interpreted the SEM microstructural results in terms of pore size distribution and chemical linking of sol particles. In the present experiments, the optimum  $C$  values for obtaining monolithic and transparent aerogels have been found to be between  $6 \times 10^{-3}$  to  $5 \times 10^{-2}$  N.

The effect of MeOH:TMOS molar ratio,  $A$ , on the aerogel microstructures has been studied by fixing the molar ratios of H<sub>2</sub>O:TMOS and NH<sub>4</sub>OH:TMOS at 4 and  $8 \times 10^{-3}$ , respectively. It has been found that as the  $A$  value increases, excess MeOH separates the molecular species formed and hinders the progress of

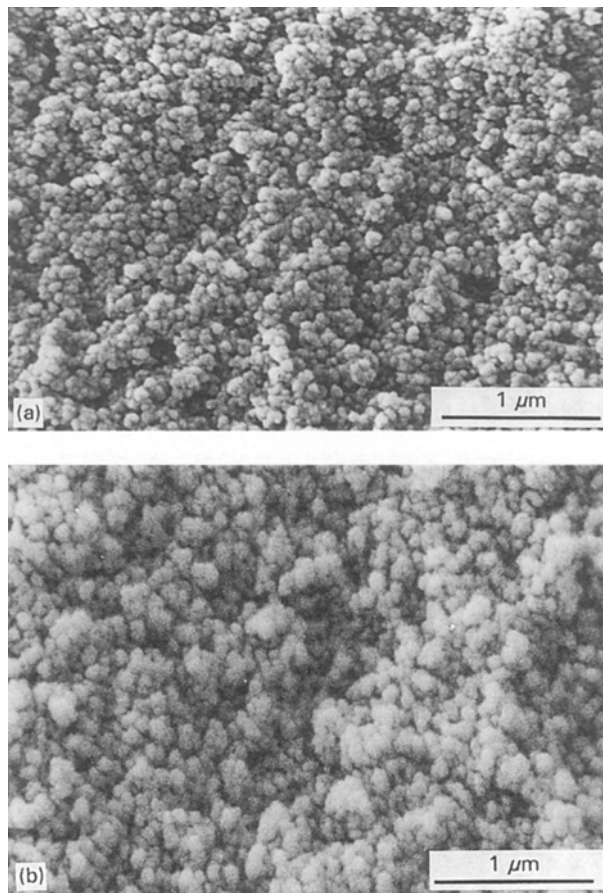


Figure 2 SEM microstructures of silica aerogels obtained using two different NH<sub>4</sub>OH:TMOS molar ratios: (a)  $4 \times 10^{-1}$  and (b)  $5 \times 10^{-3}$ .

crosslinkage of the siloxane chains leading to the separation of SiO<sub>2</sub> clusters in the sol. This process leads to a decrease in condensation reactions and hinders the formation and growth of the gel network particles, resulting in smaller particles and larger pore sizes. Fig. 3a and b shows the SEM microstructures of aerogels obtained at lower (six) and higher (18)  $A$  values, respectively. The highly crosslinked polymer network, with interconnected particles of diameters varying from 50 to 100 nm similar to several chains formed with interconnected beads, is shown for low density ( $0.05 \text{ gm cm}^{-3}$ ) aerogels, in Fig. 3b. On the other hand, high density ( $> 0.1 \text{ gm cm}^{-3}$ ) aerogels (Fig. 3a) show a continuous arrangement of particles resulting in an interconnected band structure which is similar to the structures reported in [29,42]. The particles are more or less loosely bound in a three-dimensional network. From the SEM micrographs, it can be determined that the smallest particle sizes are less than 50 nm. A variation of particle sizes can also be observed in the SEM micrographs.

The aerogels prepared using the combination of precursor (TMOS):solvent (MeOH):catalyst (NH<sub>4</sub>OH) in the molar ratio of 1:5:4:  $1 \times 10^{-2}$ , respectively, were aged for various periods ranging from 20 min to 40 days. It has been found that as the gel ageing increases, monolithicity of the aerogels also increases. Immediately after the alcogel sets, the size of the particles, and also the contact area between the particles, is rather small. Fig. 4a and b shows the SEM

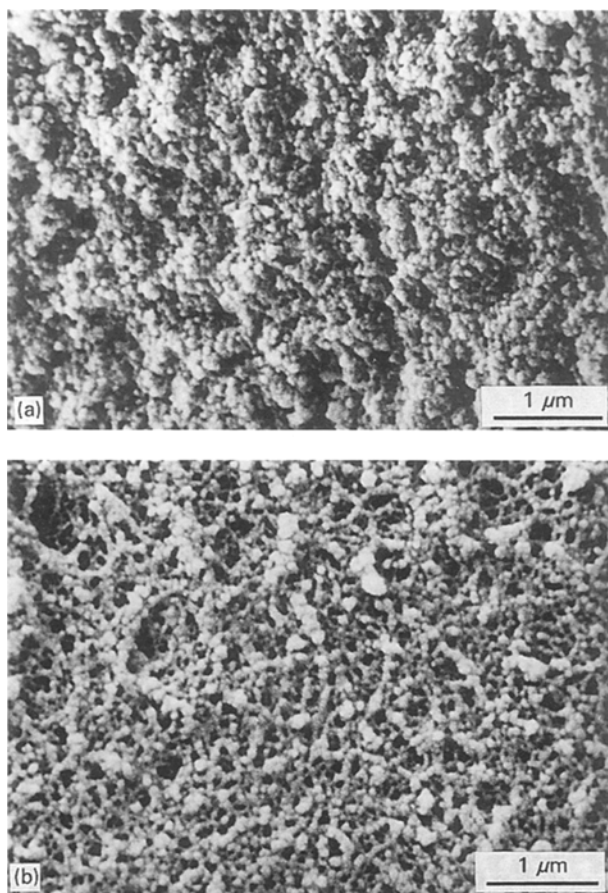


Figure 3 SEM pictures of silica aerogels produced using two different MeOH:TMOS molar ratios: (a) six, and (b) 18.

micrographs of the TMOS aerogels produced with two and 20 days gel ageing periods, respectively. The gels aged for less than five days resulted in multiple cracked aerogels, whereas monolithic aerogels were obtained with the alcogels aged for more than five days. This is due to the fact that as gel ageing increases neck growth occurs between the particles, which makes the alcogel more resistant to drying stresses. The isolated particles for two day aged gels and the neck growth between the particles for 20 day aged gels are clearly seen in Fig. 4a and b.

The autoclave heating rates and the solvent evacuation rates were varied from 8 to 200 °C h<sup>-1</sup> to 0.4–10 ml min<sup>-1</sup>, respectively. It has been found that the lower and higher heating (< 15 °C h<sup>-1</sup> and > 60 °C h<sup>-1</sup>) and evacuation (< 2 ml min<sup>-1</sup> and > 7 ml min<sup>-1</sup>) rates resulted in cracked and shrunken (10–15 vol. %) aerogels; whereas monolithic aerogels were obtained for intermediate values. Fig. 5a–c shows the SEM micrographs for higher (> 60 °C h<sup>-1</sup> and 8 ml min<sup>-1</sup>), medium (20–30 °C h<sup>-1</sup> and 4 ml min<sup>-1</sup>) and lower (< 15 °C h<sup>-1</sup> and 2 ml min<sup>-1</sup>) heating and solvent evacuation rates, respectively. The SEM results reveal that the particle sizes are larger and they are almost uniformly distributed at medium heating and solvent evacuation rates than at lower and higher rates. Moreover, the uniform packing density of the particles results in more rigidity and thereby strengthening of the gel network, leading to monolithic aerogels.

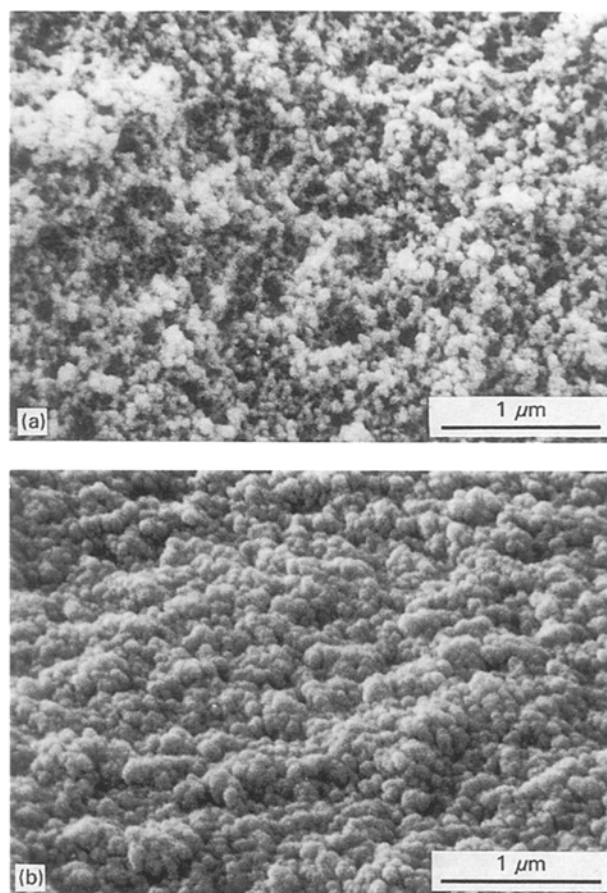


Figure 4 SEM micrographs of silica aerogels aged for (a) two days, and (b) 20 days.

As the alcogel heats in the autoclave, stresses are created in the gel because of differences in the thermal expansion coefficient between the solid gel network and the liquid in the pores of the gel [43]. The thermal expansion coefficient of the liquid is much higher than that of the gel network. The expansion creates a pressure gradient throughout the gel, because the liquid at the open end of the gel can readily establish equilibrium while the liquid at the closed end of the cylinder is not free to exit. Due to a pressure gradient, the liquid can flow from the surface of the gel, and this flux partially offsets increasing pressure created by the raising temperature, but the flux is limited by the permeability of the gel [44].

According to Darcy's law [37], the flux of liquid,  $J$ , is proportional to the pressure gradient,  $\nabla P$ , in the liquid

$$J = \frac{D}{\eta_l} \nabla P$$

where  $D$  is the permeability,  $\eta_l$  is the viscosity of the pore liquid and  $P$  is the pressure in the pore liquid.

At higher heating rates (> 60 °C h<sup>-1</sup>), the increase in pressure gradient can produce significant stresses which result in cracking and fracture of the aerogels. On the other hand, at very low heating rates (< 15 °C h<sup>-1</sup>), even though the pressure gradient decreases and the expanding liquid escapes from the gel, at the same time true expansion of the gel network results in stresses and hence cracks in the aerogels

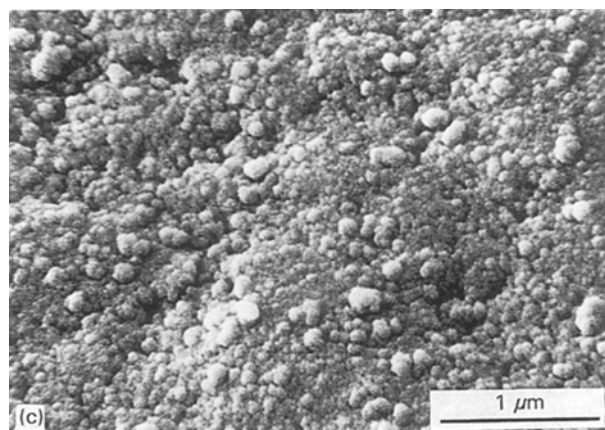
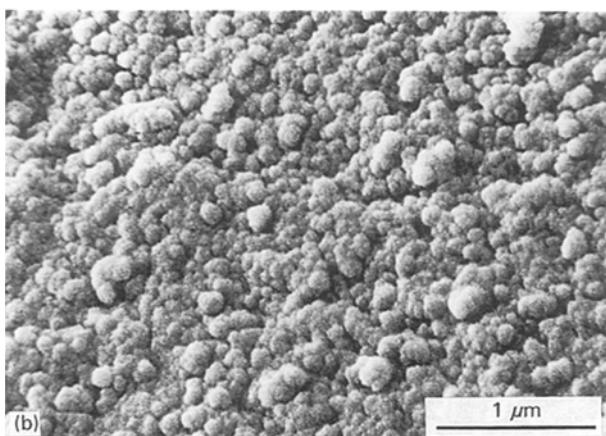
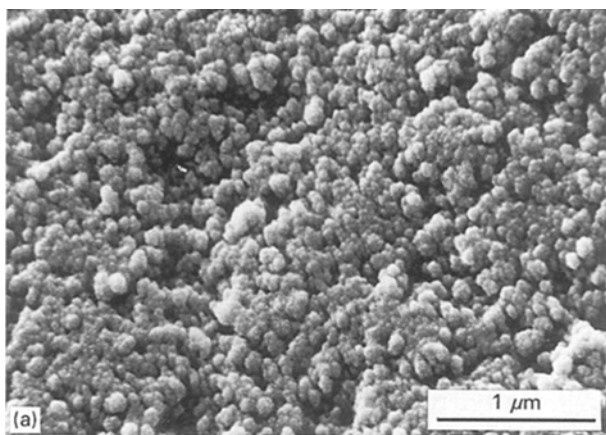


Figure 5 SEM microstructures of silica aerogels obtained for different heating and evacuation rates: (a)  $60\text{ }^{\circ}\text{C h}^{-1}$  and  $8\text{ ml min}^{-1}$ , (b)  $30\text{ }^{\circ}\text{C h}^{-1}$  and  $4\text{ ml min}^{-1}$ , and (c)  $15\text{ }^{\circ}\text{C h}^{-1}$  and  $2\text{ ml min}^{-1}$ .

because of differences in the thermal expansion coefficients of test tubes made of pyrex (low expansion) and the gels (pure silica, which has a high expansion).

In addition to the thermal stresses produced in the aerogels, the micrograph (Fig. 5c) seems to suggest that there is a greater ageing effect in the very slowly heated/evacuated gel. However, at moderate heating rates between  $20$  and  $30\text{ }^{\circ}\text{C h}^{-1}$ , monolithic and transparent aerogels have been obtained. This may be due to the fact that at these heating rates the stresses due to both the pressure gradients in the gels and the true expansion of the gels are less compared to the stresses at higher ( $> 60\text{ }^{\circ}\text{C h}^{-1}$ ) and lower ( $< 15\text{ }^{\circ}\text{C h}^{-1}$ ) heating rates, respectively.

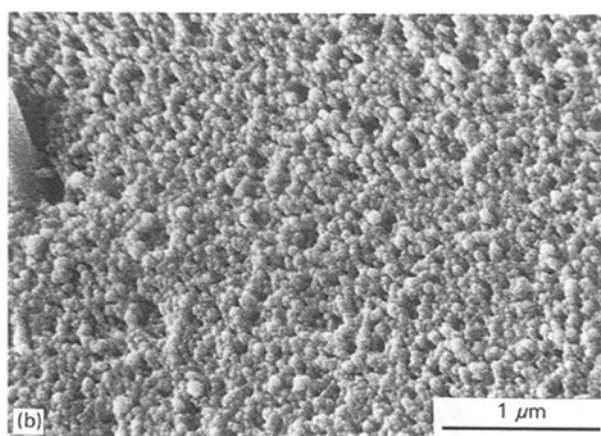
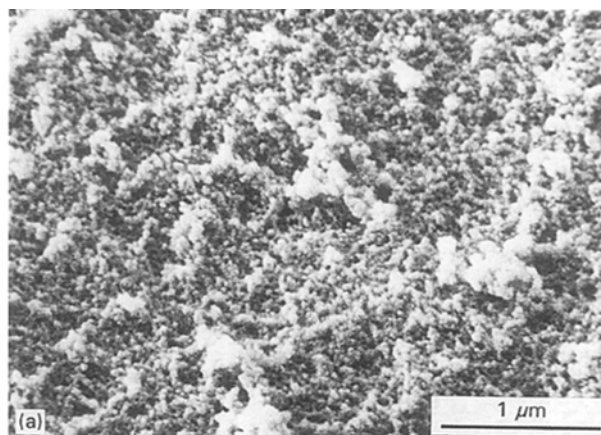


Figure 6 SEM photographs of silica aerogels prepared by (a) TEOS precursor (with HCl catalyst), and (b) TMOS precursor (with  $\text{NH}_4\text{OH}$  catalyst).

Fig. 6a and b shows SEM microstructures of the aerogels prepared using TEOS precursor with  $0.01\text{N}$  ( $0.07\%$ ) HCl ( $\text{pH} = 4$ ) and TMOS precursor with  $0.01\text{N}$  ( $0.07\%$ )  $\text{NH}_4\text{OH}$  ( $\text{pH} = 6$ ) catalysts, respectively. The molar ratios of precursor, solvent and  $\text{H}_2\text{O}$  were  $1:5:7$  and  $1:5:4$  in the former and latter cases, respectively. In the case of TEOS precursor, basic catalysts resulted in turbid sols and gels, and opaque aerogels; whereas strong acidic (excluding HCl) catalysts resulted in transparent and monolithic aerogels [24]. On the other hand, for TMOS precursor, acidic catalysts resulted in longer gel setting times and cracked aerogels; but monolithic and transparent aerogels have been obtained using weak basic (excluding  $\text{NH}_4\text{OH}$ ) catalysts [25]. It has been found that the TEOS aerogels are denser than the TMOS aerogels because of slight shrinkage ( $5\text{--}10\text{ vol } \%$ ) during supercritical drying in the former case. Clearly, the structures of TEOS (acidic) and TMOS (basic) aerogels are very different. It is clear from Fig. 6a that in the case of TEOS aerogels, the size distribution of grains is narrow and can be considered as monodispersed. However, the size distribution of clusters of grains and pores (macropores) separating these clusters is clearly polydispersed. On the other hand, TMOS aerogels (Fig. 6b) contain closely bound and almost monodispersed spherical particles with polydispersed porosity. Fig. 7 shows a few monolithic and transparent ( $85\%$  at  $900\text{ nm}$  wavelength of light for

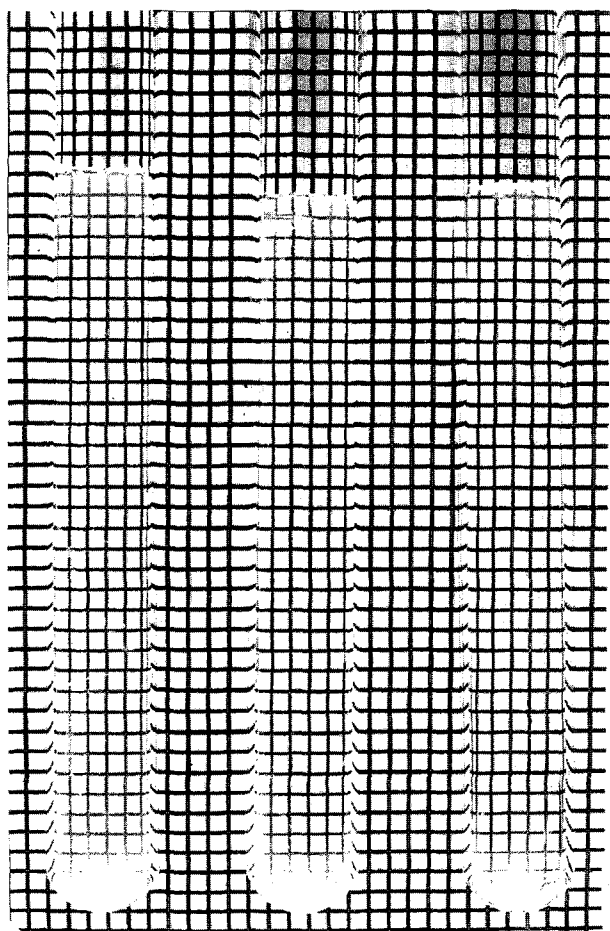


Figure 7 A few transparent monolithic silica aerogels.

a 1 cm thick sample) TMOS precursor silica aerogels obtained using an  $\text{NH}_4\text{OH}$  catalyst.

#### 4. Conclusions

From SEM microstructural observations of silica aerogels prepared using various sol-gel and supercritical drying conditions, it has been found that the strong acidic catalysed gels result in cracked but highly transparent (90% at a light wavelength of 900 nm for a 1 cm thick sample) aerogels owing to smaller particle and pore sizes. On the other hand, monolithic and slightly less transparent (85% at a wavelength of 900 nm for a 1 cm thick sample) aerogels have been obtained for basic catalysed gels. The highly cross-linked network structure of the aerogels can easily be seen at solvent/precursor molar ratios greater than 15; and below this ratio, growth of  $\text{SiO}_2$  particles occurs, which leads to monolithic aerogels. It has been observed that as the concentration of the catalyst increases, the particle and pore sizes decrease resulting in cracked but transparent aerogels. Gel ageing increases the monolithicity of silica aerogels by the formation of neck growth between the  $\text{SiO}_2$  particles. An autoclave heating rate of around  $25^\circ\text{C h}^{-1}$  and a solvent evacuation rate of  $4\text{ ml min}^{-1}$  resulted in crack-free aerogels. It has been found that TMOS precursor aerogels with a basic catalyst ( $\text{NH}_4\text{OH}$ ) show a more uniform particle size and closely bound structure with negligible shrinkage, compared to the TEOS precursor aerogels with an acid catalyst ( $\text{HCl}$ ).

#### Acknowledgements

The authors are grateful to Professor G. N. Navaneet and Mr S. V. Rao, Regional Sophisticated Instrumentation Centre (RSIC) Nagpur University, India, for help in taking the SEM micrographs. They are very thankful to Dr S. Banerjee, Head of the Metallurgy Division, BARC, Bombay, India, for helpful discussions. This work was supported by the Department of Atomic Energy (Materials Science Committee, BRNS, Project No. 34/12/90-G), Government of India. One of the authors (A. V. Rao) is most grateful to the Region Rhone-Alpes Foundation (France), for a Visiting Professorship.

#### References

1. R. POOL, *Science* **247** (1990) 807.
2. C. A. M. MULDER and J. G. VAN LIEROP, in "Proceedings of First International Symposium on Aerogels", edited by J. Fricke (Springer-Verlag, Berlin, 1986) p. 68.
3. G. M. PAJONK and C. R. INOVA, "Industrie et Innovation (France)", **18** (1976) p. 376.
4. G. M. PAJONK and S. J. TEICHNER, in "Proceedings of First International Symposium on Aerogels", edited by J. Fricke (Springer-Verlag, Berlin, 1986) p. 193.
5. A. EL TANANY and G. M. PAJONK, *React. Kinet. Catal. Lett.* **47** (1992) 167.
6. G. M. PAJONK, *Appl. Catal.* **72** (1991) 217.
7. J. FRICKE and A. EMMERLING, "Structure and Bonding 77" (Springer-Verlag, Berlin, 1992) p. 38.
8. D. W. COOPER, *Part. Sci. Technol.* **7** (1989) 371.
9. A. V. RAO, Internal Report AGL-4295 Shivaji University, Kolhapur (1995).
10. J. L. RASMUSSEN, in Proceedings of the second International Symposium on Aerogels, *Revue de Physique Appliquées, Colloque C4*, (Les Editions de Physique, Les Ulis Cedex, 1989) p. 221.
11. J. FRICKE, M. C. ARDUINI-SCHUSTER, D. BUTTNER, H. P. EBERT, U. HEINEMANN, J. HETFLEISCH, E. HUMMER, J. KUHN and X. LU, 21st International Thermal Conductivity Conference, 15–18 October, 1989, Lexington, KY.
12. J. FRICKE, *Phys. in Unserer Zeit.* **20** (1989) 189.
13. M. CANTIN, M. CASSE, L. KOCH, R. JOUAN, P. MESTREAU, D. ROUSSEL, F. BONNIN, J. MOUTEL and S. J. TEICHNER, *Nucl. Instrum. Meth.* **118** (1974) 177.
14. M. BOURDINAUD, J. B. CHEZE and J. C. THEVENIN, *ibid.* **136** (1976) 99.
15. P. J. CARLSON, K. E. JOHANSSON, J. KESTEMAN, J. NORSEBY, O. PINGOT, S. TAVERNIER, F. VAN DEN BOGAERT and L. VAN LANCKER, *ibid.* **160** (1979) 407.
16. M. GONAUER and J. FRICKE, *Acustica* **59** (1986) 177.
17. N. K. KIM, D. A. PAYNE and R. S. UPADHYE, *J. Vac. Sci. Technol.* **A7** (1989) 181.
18. K. Y. JANG, K. KIM and R. S. UPADHYE, *ibid.* **A8** (1990) 1732.
19. K. KIM, K. Y. JANG and R. S. UPADHYE, *J. Amer. Ceram. Soc.* **74** (1991) 1987.
20. C. S. ASHLEY, S. T. REED, C. J. BRINKER, R. J. WALCO, R. E. ELLEFSON and J. T. GILL in "Chemical Processing of Advanced Materials", edited by L. L. Hench and J. K. West (J Wiley, New York, 1992) p. 989.
21. S. S. KISTLER, *Nature* **127** (1931) 741.
22. G. A. NICOLAON and S. J. TEICHNER, *Bull. Soc. Chim. Fr.* **5** (1968) 1900.
23. L. W. HRUBESH, *Chem. & Ind.* 17 December, **26** (1990) 824.
24. A. V. RAO and N. N. PARVATHY, *J. Mater. Sci.* **28** (1993) 3021.
25. A. V. RAO, G. M. PAJONK and N. N. PARVATHY, *ibid.* **29** (1994) 1807.
26. A. V. RAO, G. M. PAJONK and N. N. PARVATHY, *J. Sol-Gel Sci. Technol.* **3** (1994) 205.

27. G. W. SCHERER, *J. Non-Cryst. Solids* **145** (1992) 33.
28. P. H. TEWARI, A. J. HUNT, J. G. LIEBER and K. LOFTUS, in "Proceedings of First International Symposium on Aerogels", edited by J. Fricke (Springer-Verlag, Berlin, 1986) p. 145.
29. G. POELZ, *ibid.* p. 177.
30. E. DUVAL, A. BOUKENTER, T. ACHIBAT and B. CHAMPAGNON, *Phil. Mag.* **B65** (1992) 181.
31. J. L. ROUSSET, A. BOUKENTER, B. CHAMPAGNON, J. DUMAS, E. DUVAL, J. F. QUNSON and J. SERUGHETTI, *J. Phys. Condens. Matter* **2** (1990) 8445.
32. R. W. PEKALA and C. T. ALVISO, *Mater. Res. Soc. Symp. Proc.* **180** (1990) 791.
33. L. C. KLEIN and G. J. GARVEY, *J. Non-Cryst. Solids* **38 & 39** (1980) 45.
34. C. J. BRINKER, K. D. KEEFER, D. W. SCHAEFER, R. A. ASSINK, B. D. KAY and C. S. ASHLEY, *ibid.* **48** (1982) 47.
35. M. NOGAMI and Y. MORIYA, *ibid.* **37** (1980) 191.
36. S. SAKKA, H. KOZAKA and S. KIM, in "Ultrastructure Processing of Advanced Ceramics", edited by J. D. Mackenzie and D. R. Ulrich (Wiley, New York, 1988) p. 159.
37. A. E. SCHEIDEGGER, "The Physics of Flow Through Porous Media", 3rd Edn. (University of Toronto Press, 1974) pp. 1-141.
38. P. M. ADLER, *Phys. Fluids* **29** (1986) 15.
39. G. W. SCHERER and R. W. SWAITEK, *J. Non-Cryst. Solids* **113** (1989) 119.
40. M. PRASSAS, J. PHALIPPOU and J. ZARYCKI, *J. Mater. Sci.* **19** (1984) 1656.
41. R. W. PEKALA, *ibid.* **24** (1989) 3221.
42. F. J. BROECKER, W. HECKMANN, F. FISCHER, M. MIELKE, J. SCHROEDER and A. STANGE, in "Proceedings of the First International Symposium on Aerogels", edited by J. Fricke (Springer-Verlag, Berlin, 1986) p. 160.
43. G. W. SCHERER, H. HDACH and J. PHALIPPOU, *J. Non-Cryst. Solids* **130** (1991) 157.
44. G. W. SCHERER, *ibid.*, **113** (1989) 107.

*Received 25 April 1995  
and accepted 18 March 1996*